

Poorly differentiated salivary gland carcinoma with prominent squamous metaplasia in a pregnant Wistar Hannover rat

Yuko SHIMADA¹⁾, Toshinori YOSHIDA^{2)*}, Naofumi TAKAHASHI¹⁾, Satoshi AKEMA¹⁾, Katsumi SOMA¹⁾, Aya OHNUMA-KOYAMA¹⁾, Akira SATO¹⁾, Maki KUWAHARA¹⁾ and Takanori HARADA¹⁾

¹⁾Laboratory of Pathology, Toxicology Division, The Institute of Environmental Toxicology, Uchimoriya-machi 4321, Joso-shi, Ibaraki 303-0043, Japan

²⁾Laboratory of Pathology, Tokyo University of Agriculture and Technology, 3-5-8 Saiwai-cho, Fuchu-shi, Tokyo 183-8509, Japan

(Received 14 September 2015/Accepted 5 January 2016/Published online in J-STAGE 18 January 2016)

ABSTRACT. A subcutaneous pale brown-colored mass was observed macroscopically in the ventral neck of a 16-week-old Wistar rat on day 18 of gestation. The mass was well demarcated from the adjacent tissues with partial invasion into connective tissues. Necrosis and hemorrhage were evident throughout the mass. The mass comprised a diffuse sheet and a nest-like structure of epithelial cells with prominent squamous metaplasia. The neoplastic cells tested immunopositive for keratin, vimentin, glial fibrillary acidic protein and p63. A portion of the neoplastic cells exhibited a similar immunoreaction of prominin-1 to the ductal and acinar cells in normal submandibular and parotid glands. Collectively, the tumor was diagnosed as a poorly differentiated carcinoma derived from epithelial/myoepithelial lineages in the submandibular and/or parotid glands.

KEY WORDS: carcinoma, immunohistochemistry, rat, salivary gland

doi: 10.1292/jvms.15-0539; *J. Vet. Med. Sci.* 78(5): 859–862, 2016

Salivary gland tumors often develop in rats exposed to carcinogens, such as 9,10-dimethyl-1,2-benzanthracene [3, 4, 16, 17], 2-amino-1-methyl-6-phenylimidazo [4,5-b] pyridine (PhIP) [15], isoprenaline sulphate/N-methyl-N-nitrosoarea [12] and irradiation [10]. Induced tumors exhibit various morphological phenotypes, such as squamous cell carcinoma [4, 16], well-differentiated epidermoid carcinoma [3], adenocarcinoma combined with fibrosarcoma [17] and carcinosarcoma [16]. In contrast, spontaneous salivary gland tumors are less frequently reported in relatively young adult-aged rats. A 6-week-old female Sprague-Dawley (SD) rat developed a tumor in close proximity to the parotid gland; the tumor comprised pankeratin-positive undifferentiated cells forming clusters or sheet-like structures and well-defined nests around vessels [14]. A 10-week-old male SD rat also showed a poorly differentiated carcinoma that had developed in the submandibular gland; the tumor cells tested positive for keratin and/or vimentin and possessed epithelial/mesenchymal (bipotential) cell lineages [11]. A similar case, diagnosed as epithelial-myoepithelial carcinoma, was reported in a 21-week-old male SD rat [8]. In the present case report, we describe the histological characteristics of a poorly differentiated carcinoma with a suspected salivary gland origin in a pregnant 16-week-old Wistar BrlHan:WIST@Jcl (GALAS) rat.

The affected animal was a specific pathogen-free female BrlHan:WIST@Jcl (GALAS) rat purchased at the age of 13 weeks from the Fuji Breeding Center (CLEA Japan, Inc., Hamamatsu, Japan) and housed in a barrier-sustained animal room at controlled temperature ($22 \pm 2^\circ\text{C}$), humidity ($50 \pm 20\%$), ventilation (at least 10 times/hr, on an all-fresh-air basis) and illumination (12 hr/day, light on at 07:00 and off at 19:00). The animal was housed in a suspended wire-mesh stainless steel cage (310 mm width \times 440 mm diameter \times 230 mm height) during the acclimatization period and then moved to an aluminum cage with a wire-mesh floor and front (260 mm width \times 400 mm diameter \times 240 mm height) for mating. The rat was handled in accordance with the Guidelines for Animals Experimentation issued by the Japanese Association for Laboratory Animal Science and the Code of Ethics for Animal Experimentation of this institute.

The neoplastic mass was fixed in 10% neutral-buffered formalin and routinely embedded in paraffin. The paraffin sections (5 μm) were stained with hematoxylin and eosin, Alcian blue and Masson's trichrome or periodic acid-Schiff, with or without diastase treatment. Immunohistochemical analysis was performed in paraffin sections using the Dako EnVision kit (Dako, Glostrup, Denmark). Sections were incubated with one of the following primary antibodies: anti-cow keratin antibody (fully diluted), anti-CK19 antibody ($\times 50$), anti-pig vimentin monoclonal antibody (V9, $\times 50$), anti-human p63 antibody ($\times 100$), anti-cow glial fibrillary acidic protein (GFAP) antibody (fully diluted), anti-chicken desmin antibody (fully diluted), anti-cow S-100 protein polyclonal antibody ($\times 400$), anti-rat proliferating nuclear cell antigen (PCNA) monoclonal antibody (PC10, $\times 1,000$), anti-human prominin-1 antibody ($\times 100$), anti-human chromogranin A polyclonal antibody ($\times 200$) and anti-human synaptophysin antibody (fully diluted). We also used a horseradish perox-

*CORRESPONDENCE TO: YOSHIDA, T., Laboratory of Veterinary Pathology, Tokyo University of Agriculture and Technology, 3-5-8 Saiwai-cho, Fuchu-shi, Tokyo 183-8509, Japan.
e-mail: yoshida7@cc.tuat.ac.jp

©2016 The Japanese Society of Veterinary Science

This is an open-access article distributed under the terms of the Creative Commons Attribution Non-Commercial No Derivatives (by-nc-nd) License <<http://creativecommons.org/licenses/by-nc-nd/4.0/>>.

idase-labeled anti-human α -smooth muscle action (α SMA) monoclonal antibody (1A4, $\times 100$). The primary antibodies for CK19 and prominin-1 were obtained from Roche Diagnostics Ltd. (Basel, Switzerland) and Abnova Corporation (Taipei, Taiwan), respectively, while the remaining antibodies were obtained from Dako. For antigen retrieval, sections were pretreated with sodium citrate buffer (0.1 M, pH 6.0) in an autoclave at 121°C for 5 min. Sections stained without primary antibodies were used as negative controls. The immunohistochemical products were visualized using the substrate 3,3'-diaminobenzidine and counterstained with hematoxylin. Antibody specificities were confirmed in internal tissues, such as epidermis, subcutaneous tissues and salivary glands (acinar cells and myoepithelial cells).

In the clinical evaluation, a subcutaneous mass was found in the ventral neck on day 18 of gestation. The rat was deeply anesthetized with ether and then euthanized by exsanguination. During necropsy, a subcutaneous pale brown-colored mass of approximately 30 mm in diameter was found in the ventral neck, and normal submandibular and parotid glands were closely attached to the subcutaneous mass. The cut surface of the mass was whitish or brownish in color with a lobular structure including necrotic or hemorrhagic foci (Fig. 1A and 1B). Microscopically, the mass was well demarcated from the adjacent tissues, such as the epidermis (Fig. 2A), with slight compression of the residual submandibular and parotid glands. Partial invasion into connective tissues was noted; however, no evidence of metastasis to other organs, including the regional lymph node, was observed. The major part of the mass comprised a diffuse sheet of poorly differentiated epithelial-like cells, in which acinar or ductal structure was extremely limited (Fig. 2B). Some of the peripheral cells were arranged in a nest-like structure (Fig. 2C). In both areas, the neoplastic cells comprised irregularly-shaped nuclei with prominent nucleoli, basophilic cytoplasm and distinct cell membrane. Mitotic figures and apoptosis were frequently observed. Foci of squamous metaplasia (Fig. 2D), necrosis, hemorrhage and interstitial vascularization were present throughout the mass.

Immunohistochemically, the neoplastic cells tested positive for keratin (an epithelial marker) (Fig. 3A) and vimentin (a mesenchymal marker) (Fig. 3B). A relatively small proportion of neoplastic cells were also positive for GFAP (a myoepithelial marker) (Fig. 3C), while the nuclei in neoplastic cells were highly positive for p63 (a myoepithelial marker) (Fig. 3D). A small number of neoplastic cells were positive for CK19 (an epithelial cell marker at a low molecular weight), α SMA (a myoepithelial or smooth muscle cell marker), desmin (a myoepithelial, smooth or skeletal muscle cell marker) and prominin-1 (a marker for intercalated ducts and acinar cells) (Fig. 3E). Negative reactions for synaptophysin and chromogranin A (neuroendocrine markers) were detected in almost all tumor cells. In foci of squamous metaplasia, squamous cells were positive for keratin, and surrounding tumor cells were positive for keratin, CK19, p63 and S-100 (a Schwann cell or myoepithelial cell marker). Cell proliferation activity was extremely high in the tumor cells, as indicated by PCNA immunostaining

(Fig. 3F). In the normal submandibular and parotid glands, positive reactions for keratin and prominin-1 (Fig. 3E, inset) were detected in ductal and acinar cells, while positive reactions for vimentin, GFAP, p63 and S-100 were detected in myoepithelial cells.

Spontaneous salivary gland tumors are extremely rare in commonly-utilized rats. A spontaneous papillary cystadenocarcinoma in the parotid gland with histomorphologic characteristics of cystic and papillary growth was previously reported in a 72-week-old F344 rat [7]. The tumor cells were cuboidal to tall columnar epithelium with mucoid, pale cytoplasm and medium to large nuclei; however, myoepithelium-like tumor cells did not appear to be associated with the tumor cysts and the papillae. In contrast, the present case was closely similar to two previous cases of SD rats that exhibited poorly-differentiated tumor cells with a diffuse sheet or nest-like structure [8, 11]. Immunohistochemically, the tumor cells in these cases tested positive for epithelial cell markers (such as keratin, AE1/3 and/or epithelial membrane antigen) and myoepithelial cell markers (such as vimentin, α SMA, GFAP and/or p63). These histopathological and immunohistochemical phenotypes of both tumor cells were almost consistent with our findings: the tumor cells tested positive for epithelial and myoepithelial cell markers, although they could not be subdivided into epithelial or myoepithelial cells on H&E-stained sections. Epithelial-myoepithelial carcinoma is characterized by proliferation of luminal epithelial cells surrounded by clear myoepithelial cells [9]; however, our case lacked double-layered pattern of epithelial cells and myoepithelial cells. Therefore, the most appropriate term for diagnosis of the present case would be poorly-differentiated carcinoma rather than epithelial-myoepithelial carcinoma. It is relatively rare for pathologists to find a spontaneous tumor in pregnant female rats. Such a poorly-differentiated salivary gland tumor, as reported in relatively young adult-aged rats [8, 11, 14], may have incidentally developed in the pregnant female Wistar rat in the current case report.

The tumor mass in our case often contained foci of squamous metaplasia; to the best of our knowledge, this has been unreported in spontaneously-occurred and induced salivary gland tumors in rats; however, it was experimentally induced by arterial ligation of rat submandibular and sublingual salivary glands [2]. Early stages of this process involved a gradual dedifferentiation of acinar cells and hyperplasia of the acinar, duct luminal cells and myoepithelium. Subsequently, in both luminal and myoepithelial cells, the accumulation of tonofilaments and the formation of desmosomes increased, and centrally located acinar-intercalated duct complexes may have undergone keratinization, i.e., squamous metaplasia. This process is believed to have important connotations for salivary gland tumors, such as pleomorphic adenoma [6] and mucoepidermoid carcinoma [1] with squamous metaplasia in humans. Given that the basaloid epithelial and myoepithelial cells surrounded foci of squamous metaplasia, those might be generated from both types of tumor cells. The abnormal intratumoral environment in our case may have caused the remarkable appearance of the squamous metaplasia, as similarly reported in human salivary gland tumors.

Fig. 1

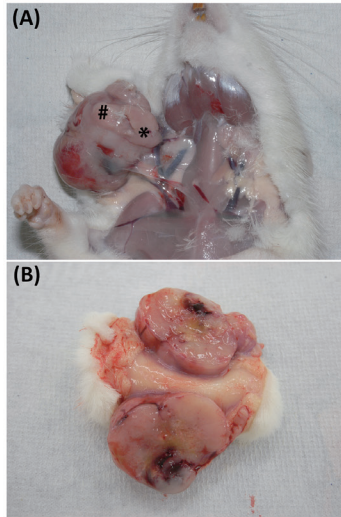


Fig. 2

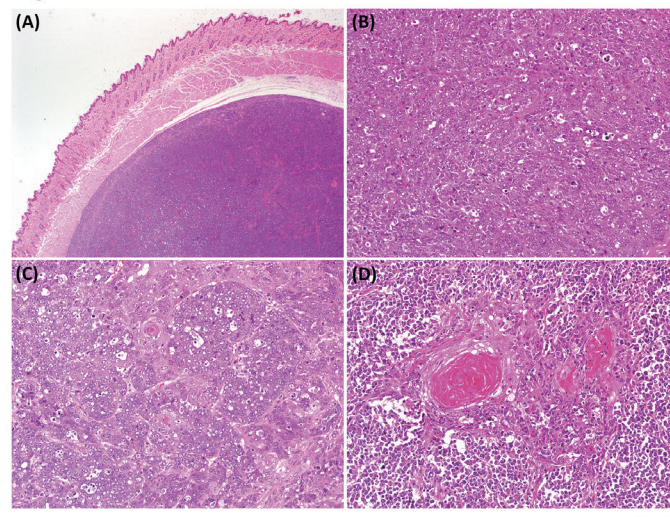


Fig. 3

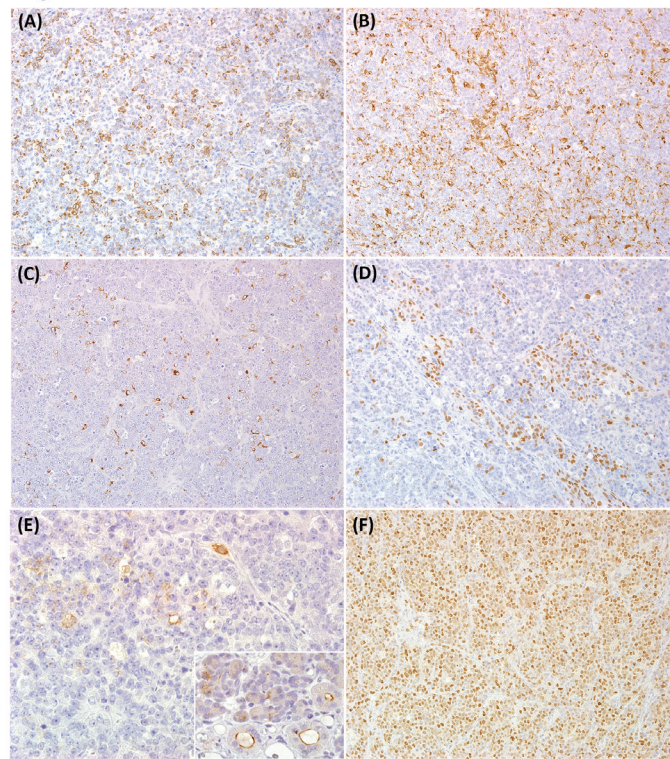


Fig. 1. Macroscopic findings in the salivary gland tumor. (A) A pale brown-colored mass in close proximity to the submandibular (asterisk) and parotid glands (sharp). (B) Tumor exhibits a solid pattern with a pale brown-colored lobular structure and necrotic and hemorrhagic foci.

Fig. 2. Histopathological findings in the salivary gland tumor. (A) The tumor tissue is located below the cutaneous muscle and demarcated by a loose connective tissue. (B) The tumor is composed of a solid growth of homogenous tumor cells with prominent apoptosis. (C) The tumor cells are arranged in a nest-like pattern of poorly differentiated epithelial-like cells, demarcated by interstitial connective tissues. Foci of squamous metaplasia are also notable. (D) Squamous metaplasia of the tumor cells. Hematoxylin and eosin staining. (A) Bar=80 μ m. (C-D) Bar=40 μ m.

Fig. 3. Immunohistochemical findings in the salivary gland tumor. Many tumor cells are positive for an epithelial marker, cytokeratin (A) and a mesenchymal cell marker, vimentin (B), while some tumor cells are positive for myoepithelial cell markers, GFAP (C) and p63 (D). (E) A small proportion of tumor cells are positive for prominin-1, a ductal and acinar cell marker. Inset: Expression of prominin-1 in ductal and acinar cells of normal parotid gland. (F) The nuclei of almost all tumor cells are labeled with PCNA. Bar=40 μ m.

In the present case, prominin-1-positive reactions were identified in a small population of tumor cells, as well as in the ductal and acinar cells in normal submandibular and parotid glands. A positive signal of prominin-1 in normal rat tissues was consistent with the findings in mouse submandibular glands [9]. The findings strongly suggested that the tumor cells in our case were derived from the salivary glands. On the other hand, prominin-1 (CD133)-positive cancer stem cells scattered in the pseudocyst-lining area of cribriform patterns exhibit a Swiss cheese-like appearance and accumulate in thin epithelial cords or trabecular arrangements in human adenoid cystic carcinoma [5]. Prominin-1-positive cells were also identified in a pleomorphic adenoma fene-1 transgenic mouse model of a salivary gland tumor [13] and in a regenerative mouse salivary gland post-irradiation damage [9]. As a positive signal of a single cell marker prominin-1 was limited in our tumor mass, it remains unknown that cancer stem cells may have played a role in the morphogenesis of the development of the salivary gland tumor in such a young-aged rat.

Collectively, we diagnosed the tumor as a poorly differentiated carcinoma derived from the epithelial and/or myoepithelial lineages in the submandibular and/or parotid glands. Although our case was observed in only one rat, expression of several cell markers would provide useful information, considering the tumor development and therapeutic target, for modeling a human salivary gland tumor with a poor prognosis.

ACKNOWLEDGMENTS. We are very grateful to Mrs. Junko Fukumori, Kayoko Iijima, Yukie Sakano, Chizuko Tomiyama, Takako Kazami, Mutsumi Kumagai and Yuko Chiba for their assistance in tissue preparation and staining.

REFERENCES

- Batrani, M., Kaushal, M., Sen, A. K., Yadav, R. and Chaturvedi, N. K. 2009. Pleomorphic adenoma with squamous and appendageal metaplasia mimicking mucoepidermoid carcinoma on cytology. *Cytojournal* **6**: 5. [Medline] [CrossRef]
- Dardick, I., Jeans, M. T., Sinnott, N. M., Wittkuhn, J. F., Kahn, H. J. and Baumal, R. 1985. Salivary gland components involved in the formation of squamous metaplasia. *Am. J. Pathol.* **119**: 33–43. [Medline]
- El-Mofty, S. 1977. Immunological studies of induced tumors of the rat submandibular gland. *Oncology* **34**: 53–57. [Medline] [CrossRef]
- Englander, A. and Cataldo, E. 1976. Experimental carcinogenesis in duct-artery ligated rat submandibular gland. *J. Dent. Res.* **55**: 229–234. [Medline] [CrossRef]
- Fujita, S. and Ikeda, T. 2012. Cancer stem-like cells in adenoid cystic carcinoma of salivary glands: relationship with morphogenesis of histological variants. *J. Oral Pathol. Med.* **41**: 207–213. [Medline] [CrossRef]
- Goulart, M. C., Freitas-Faria, P., Goulart, G. R., Oliveira, A. M., Carlos-Bregni, R., Soares, C. T. and Lara, V. S. 2011. Pleomorphic adenoma with extensive squamous metaplasia and keratin cyst formations in minor salivary gland: a case report. *J. Appl. Oral Sci.* **19**: 182–188. [Medline] [CrossRef]
- Hosokawa, S., Imai, T., Hayakawa, K., Fukuta, T. and Sagami, F. 2000. Parotid gland papillary cystadenocarcinoma in a Fischer 344 rat. *Contemp. Top. Lab. Anim. Sci.* **39**: 31–33. [Medline]
- Li, Y., Kim, H. S., Kang, M. S., Shin, S. H., Koo, K. H., Kim, C. M., Kim, K. H., Peck, C., Bae, H. I., Jeong, J. Y., Kang, J. S. and Kang, B. H. 2013. A spontaneous epithelial-myoepithelial carcinoma of the submandibular gland in a sprague-dawley rat. *J. Toxicol. Pathol.* **26**: 67–72. [Medline] [CrossRef]
- Nanduri, L. S., Maimets, M., Pringle, S. A., van der Zwaag, M., van Os, R. P. and Coppes, R. P. 2011. Regeneration of irradiated salivary glands with stem cell marker expressing cells. *Radiother. Oncol.* **99**: 367–372. [Medline] [CrossRef]
- Nicolatou, O. E. 1981. Morphologic changes in rat parotid following isoproterenol administration and fractionated x-irradiation. *J. Oral Pathol.* **10**: 311–321. [Medline] [CrossRef]
- Nishikawa, S., Sano, F., Takagi, K., Okada, M., Sugimoto, J. and Takagi, S. 2010. Spontaneous poorly differentiated carcinoma with cells positive for vimentin in a salivary gland of a young rat. *Toxicol. Pathol.* **38**: 315–318. [Medline] [CrossRef]
- Parkin, R. and Neale, S. 1976. The effect of isoprenaline on induction of tumours by methyl nitrosourea in the salivary and mammary glands of female wistar rats. *Br. J. Cancer* **34**: 437–443. [Medline] [CrossRef]
- Shen, S., Yang, W., Wang, Z., Lei, X., Xu, L., Wang, Y., Wang, L., Huang, L., Yu, Z., Zhang, X., Li, J., Chen, Y., Zhao, X., Yin, X. and Zhang, C. 2011. Tumor-initiating cells are enriched in CD44(hi) population in murine salivary gland tumor. *PLoS ONE* **6**: e23282. [Medline] [CrossRef]
- Tsunenari, I., Yamate, J. and Sakuma, S. 1997. Poorly differentiated carcinoma of the parotid gland in a six-week-old Sprague-Dawley rat. *Toxicol. Pathol.* **25**: 225–228. [Medline] [CrossRef]
- Wang, R., Dashwood, W. M., Löhr, C. V., Fischer, K. A., Pereira, C. B., Louderback, M., Nakagama, H., Bailey, G. S., Williams, D. E. and Dashwood, R. H. 2008. Protective versus promotional effects of white tea and caffeine on PhIP-induced tumorigenesis and β -catenin expression in the rat. *Carcinogenesis* **29**: 834–839. [Medline] [CrossRef]
- Watanabe, Y., Ozono, S., Sato, K., Hisada, T. and Heyden, G. 1987. The application of microspectrocytofluorometric measurement of Feulgen nuclear DNA content to experimental tumors of rat submandibular gland. 1. Pathogenesis and nuclear DNA content. *J. Oral Pathol.* **16**: 1–7. [Medline] [CrossRef]
- Zaman, A., Kohgo, T., Shindoh, M., Iizuka, T. and Amemiya, A. 1996. Induction of adenocarcinomas in the submandibular salivary glands of female Wistar rats treated with 7,12-dimethylbenz(a)anthracene. *Arch. Oral Biol.* **41**: 221–224. [Medline] [CrossRef]